Available online at www.sciencedirect.com
ScienceDirect
Journal of Nuclear Materials 363–365 (2007) 184–189
journal of nuclear materials
www.elsevier.com/locate/jnucmat

Hydrogen isotopic effects on the chemical erosion of graphite induced by ion irradiation

J.H. Liang [a,*], M. Mayer [b], J. Roth [b], M. Balden [b], W. Eckstein [b]

[a] National Tsing Hua University, Department of Engineering and System Science, Hsinchu 300, Taiwan, ROC
[b] Max-Planck-Institut für Plasmaphysik, EURATOM Association, Boltzmannstrasse 2, D-85748 Garching, Germany

Abstract

This theoretical study investigates the dynamic behavior of chemical erosion of graphite due to hydrogen-isotope ion bombardment. The ion energy ranges from 10 to 1000 eV and the target temperature ranges from 300 to 1100 K. The chemical erosion processes under investigation included surface-related and thermally activated hydrocarbon emission processes. The computer code TRIDYN was employed. The proposed simulation model was fitted to experimental data by implementing surface-related and thermally activated coefficients. It is improved compared to our previous model by incorporating a depth-dependent probability for out-diffusion of hydrocarbons. The local reduction of carbon density due to either physical sputtering or chemical erosion was also taken into account. Furthermore, the erosion for all three hydrogen isotopes – hydrogen, deuterium, and tritium – was modeled. All the calculated and fitted results are in good agreement with measured data. The results from the current simulation model surpass previous ones in the low ion energy region in which chemical erosion is of vital importance.

PACS: 61.43.Bn; 81.05.Uw; 25.60.Pj; 92.40.Gc; 32.10.Bi; 68.49.Sf

Keywords: Computer simulation; Graphite; Thermonuclear fusion; Chemical erosion; Hydrogen isotope; Physical sputtering

1. Introduction

In recent decades, the suitability of graphite as an inner-wall material in thermonuclear fusion devices [1,2] has attracted considerable interest in both theoretical simulations and experimental measurements due to its superior thermal and mechanical properties, and its good plasma compatibility. However, in addition to physical sputtering, the erosion of graphite can be greatly enhanced by chemically released volatile hydrocarbons (so-call chemical erosion) via chemical reaction between carbon and hydrogen through surface-related and thermally activated hydrocarbon emission processes [3]. The emitted hydrocarbons consist dominantly of methane molecules or methyl radicals, even if heavier hydrocarbons contribute significantly at some erosion conditions [4–10]. The surface-related process refers to ion induced release of weakly bound hydrocarbon complexes from the surface while the

* Corresponding author. Fax: +886 35720724.
E-mail address: jhliang@ess.nthu.edu.tw (J.H. Liang).

0022-3115/$ - see front matter
doi:10.1016/j.jnucmat.2007.01.006

thermally activated process refers to thermal release of hydrocarbons at the end of ion range. Chemical erosion processes can result in undesirable effects such as a limited lifetime of components, plasma dilution with impurities, and high tritium retention in re-deposited hydrocarbon layers [3]. Hence, a thorough understanding of dynamic characteristics of graphite exposed to an energetic plasma containing different hydrogen isotopes (H, D, and T) is essential before considering thermonuclear fusion for industrial applications. Additionally, a comprehensive model for simulating the chemical erosion of graphite under bombardment with hydrogen isotopes is necessary in order to gain more insight into the chemical erosion mechanisms and in designing a more suitable inner-wall material (such as doped graphites [11]). It is therefore the objective of this study to improve our previous model [12] by incorporating the diffusion model proposed by Hopf et al. [13] as well as extending its applicability to all hydrogen isotopes. Note, hydrogen is through out the paper as synonym for the three isotopes, and if it is necessary to refer to one isotope, the chemical symbols H, D, and T are used. Both chemical erosion and physical sputtering of graphite are studied depending on ion energy and target temperature.

2. Simulation model

The total erosion yield (Y_{tot}) of graphite under hydrogen ion irradiation is given by the following equation [3]:

$$Y_{\mathrm{tot}} = Y_{\mathrm{phys}} + Y_{\mathrm{chem}} = Y_{\mathrm{phys}} + Y_{\mathrm{surf}} + Y_{\mathrm{therm}}, \qquad (1)$$

where Y_{phys} denotes the physical sputtering yield of graphite due to the kinetic emission of carbon atoms from the target surface; Y_{chem} represents the chemical erosion yield of graphite due to the emission of hydrocarbons; Y_{surf} denotes the chemical erosion yield of graphite due to the emission of surface-related hydrocarbons from the target surface; Y_{therm} represents the chemical erosion yield of graphite due to the emission of thermally activated hydrocarbons from the target surface as well as from the bulk.

The current simulation model of Y_{surf} and Y_{therm} is improved compared to our previous one [12] by including an out-diffusion probability of hydrocarbons [13]. The calculated surface-related and thermally activated chemical erosion yields are given by the fluence-averaged values as follows:

$$Y_{\mathrm{surf}}^{\mathrm{calc}} = \frac{1}{\Phi}\sum_i \alpha \frac{(\mathrm{H/C})_{x_i}}{(\mathrm{H/C})_{\mathrm{max}}} f_{d,x_i} P_{\mathrm{diff},x_i} \quad \text{if } 0 \leqslant x_i \leqslant x_{\mathrm{surf}}; \qquad (2)$$

$$Y_{\mathrm{therm}}^{\mathrm{calc}} = \frac{1}{\Phi}\sum_i \beta \frac{(\mathrm{H/C})_{x_i}}{(\mathrm{H/C})_{\mathrm{max}}} Y_{\mathrm{therm}}^{\mathrm{meas}} \quad \text{if } 0 \leqslant x_i, \qquad (3)$$

where the superscripts 'calc' and 'meas' denote the calculated values yielded from this study and the measured data obtained from other studies [10,14], respectively; the subscripts 'surf' and 'therm' represent the surface-related and thermally activated processes emitting hydrocarbons, respectively; the subscript 'i' denotes the ith implanted hydrogen ion. Note, all the possible volatile hydrocarbon species, including methane molecules, methyl radicals, heavier hydrocarbons, etc. are taken into account implicitly in the current simulation model. In addition, (i) $\Phi = \phi t$ denotes the hydrogen ion fluence, ϕ represents the hydrogen ion flux, and t denotes the implantation time; (ii) α and β represent the surface-related and thermally activated coefficients, respectively, which are to be determined; (iii) $(\mathrm{H/C})_{x_i}$ refers to the atomic ratio of hydrogen to carbon at the location x_i, where it attempts to saturate to a temperature-dependent value $(\mathrm{H/C})_{\mathrm{max}}$ as ion fluence exceeds some critical fluence Φ_{crit}; (iv) $(\mathrm{H/C})_{\mathrm{max}}$ decreases exponentially from 0.42 [15–17] to approximately zero as target temperature increases from 300 to 1100 K and is assumed to be identical for all hydrogen isotopes; (v) x_i indicates the location or depth of the ith implanted hydrogen in graphite [18]; (vi) f_{d,x_i} refers to implantation damage produced at x_i [3,15,16,19]; and (vii) $P_{\mathrm{diff},x_i} = e^{-x_i/\lambda}$ refers to the depth-dependent probability of out-diffusing hydrocarbons from x_i [13]. The diffusion length λ is assumed to increase linearly with target temperature (i.e., $\lambda = 0.4$ nm at 300 K [13] and $\lambda = x_{\mathrm{surf}}$ at 1100 K); x_{surf} represents the maximum depth at which chemical erosion of graphite due to the emission of surface-related hydrocarbons from the target surface takes place and is given by 1 nm [20]. The possibility of segregation and formation of gas molecules such as H_2, D_2, or T_2 [21] in graphite is neglected in the present study.

Furthermore, the chemical erosion of graphite due to hydrogen irradiation was dynamically conducted by implementing Eqs. (2) and (3) in the dynamic Monte-Carlo computer simulation code TRIDYN [22]. The ion fluence employed was 1.25×10^{19} ions/cm^2 [1]. The ion energy (E) ranges from 10 to 1000 eV and the target temperature (T)

ranges from 300 to 1100 K. The number of simulated particles was 10^6 in all computations. In addition, an iteration procedure as well as a least-squares fitting technique were applied for best approximating $Y_{\text{chem}}^{\text{calc}}$ to $Y_{\text{chem}}^{\text{meas}}$ to determine the coefficients α and β. Note, Roth's [3] fit formula of $Y_{\text{chem}}^{\text{Roth}}$ approximates well to $Y_{\text{chem}}^{\text{meas}}$ and is thus adopted in the present study to represent $Y_{\text{chem}}^{\text{meas}}$.

Another simulation model was proposed by Hopf and Jacob [23]. Although developed independently, it is interesting to note that both models show many similarities. However, the main differences can be summarized as follows: (1) the Hopf simulation model uses the 'static' computer code TRIM.SP [24] (which is valid only for low ion fluence) to calculate both damage and implanted-ion depth profiles while the current simulation model uses the 'dynamic' computer code TRIDYN (which allows to take fluence dependent target changes into accounts and is especially applicable for high ion fluence); (2) the Hopf simulation model uses bond breaking events to represent damage depth profile while the current simulation model uses the nuclear energy deposition function (which leads to differences at low ion energies [23]); (3) the current simulation model uses an additional term of $(\text{H/C})_{x_i}/(\text{H/C})_{\max}$ to account more realistically for the variation of volatile hydrocarbon formation at the location x_i as a function of hydrogen fluence.

3. Results and discussion

The best-fitting coefficients α and β obtained from this study for graphite bombarded by hydrogen ions at various target temperatures are shown in Table 1. As can be seen, α is more dependent on target temperature than β and decreases with increasing target temperature. However, β increases moderately with increasing target temperature, peaks at 773 K, and decreases then. Both α and β depend on the isotope, where D and H ions have the largest values of α and β, respectively. The former indicates that D possesses the greatest ability to form volatile hydrocarbons [25] while the latter reveals that the largest amount of H ions is reflected from the target surface and end up at a depth that is not saturated with the $(\text{H/C})_{\max}$ value [12].

Table 1
Best-fitting coefficients α and β for graphite bombarded by hydrogen ions at various target temperatures

T (K)	α[a]			β		
	H	D	T	H	D	T
300	5.00E−3	7.14E−3	5.93E−3	1.42	1.31	1.23
473	3.78E−3	5.45E−3	4.51E−3	1.44	1.32	1.24
573	3.56E−3	5.03E−3	4.10E−3	1.46	1.33	1.24
673	3.65E−3	4.86E−3	3.87E−3	1.51	1.35	1.25
773	3.66E−3	4.64E−3	3.64E−3	1.54	1.37	1.27
873	2.64E−3	3.30E−3	2.57E−3	1.49	1.33	1.23
973[b]	7.41E−4	9.26E−4	7.22E−4	1.48	1.32	1.22
1100[b]	2.64E−5	3.30E−5	2.58E−5	1.47	1.32	1.22

[a] Calculated according to the number of hydrocarbons/(eV/nm).

[b] $(\text{H/C})^{\max}$ was assumed to be 10^{-4} for target temperatures greater than 900 K.

The dependence of the different yields (Y_{phys}, Y_{surf}, Y_{therm}) on ion energy due to D ion irradiation at target temperatures of 300 and 773 K is plotted in Fig. 1. In the figure, the solid, dashed, and dotted lines illustrate the results calculated from the current simulation model (Y^{calc}), the results calculated with the previous simulation model applied here to D (Y^{prev}) [12], and the results yielded from Roth's fit formula [3] (Y^{Roth}), respectively. Note, the ion flux employed in Roth's fit formula was 10^{16} ions/cm^2 s [1]. The surface-related and thermally activated chemical erosion processes are dominant at low and high target temperatures, respectively. The values of Y_{therm} and Y_{phys} for the current model (Y^{calc}) and the previous model (Y^{prev}) are almost the same and hard to be singled out in Fig. 1. However, there are some discrepancies between $Y_{\text{surf}}^{\text{calc}}$ and $Y_{\text{surf}}^{\text{prev}}$ especially in the low ion energy region (<40 eV), which is

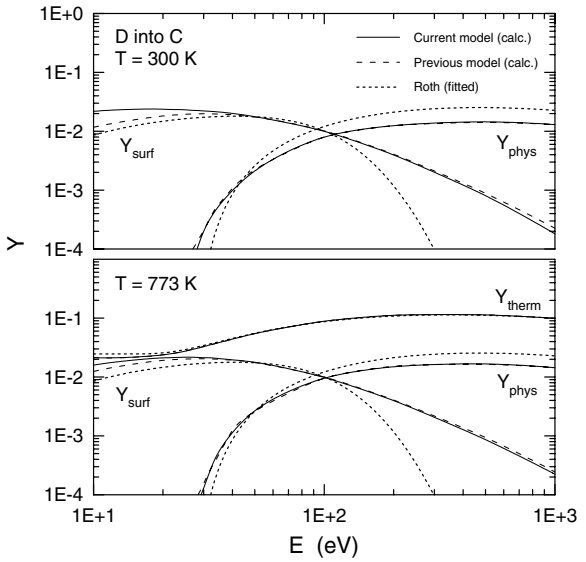

Fig. 1. Y_{surf}, Y_{therm}, and Y_{phys} as a function of ion energy for graphite bombarded by deuterium ions at target temperatures of 300 and 773 K.

mainly due to the inclusion of a depth-dependent probability for out-diffusion of hydrocarbons in the current simulation model compared to the previous simulation model. The discrepancies get larger by decreasing either ion energies (i.e., decreasing X_i) or target temperatures (i.e., increasing λ). Also note that Y_{surf}, Y_{therm}, and Y_{phys} values increase with increasing ion mass.

Also shown in Fig. 1, all of the Y^{calc}_{surf}, Y^{calc}_{therm}, and Y^{calc}_{phys} values reproduce the corresponding Y^{Roth} values quite well. However, there are some discrepancies between Y^{calc}_{surf} and Y^{Roth}_{surf} and between Y^{calc}_{phys} and Y^{Roth}_{phys}. Differences in Y_{surf} arise at both, lower ($E < 40$ eV) and higher ion energies ($E > 100$ eV). Note, Y^{Roth}_{surf} was obtained by fitting it to the measured data Y^{meas}_{surf}. For lower ion energies, a further comparison of Y^{calc}_{surf} and Y^{Roth}_{surf} with Y^{meas}_{surf} is needed and will be discussed in Fig. 2. For higher ion energies, Y^{calc}_{surf} is much smaller than Y^{calc}_{phys} and the fitting error may be substantial for small values, this discrepancy can be disregarded [12].

The differences in Y_{phys} are primarily due to that fact that Roth's fit formula for Y_{phys} is derived with the underlying assumption that the graphite target material does not change its C concentration during D ion bombardment. In reality, D ion irradiation causes a reduction of the C fraction in the target material, subsequently resulting in a decrease of Y^{calc}_{phys} when compared to Y^{Roth}_{phys}. In addition, (D/C)$_{max}$ increases (i.e., the atomic fraction of carbon decreases) as target temperature decreases. Hence, the difference between Y^{calc}_{phys} and Y^{Roth}_{phys} gets larger at decreasing target temperatures. Similar phenomena occur for H and T ion bombardment. The discrepancy between Y^{calc}_{phys} and Y^{Roth}_{phys} increases as ions become heavier.

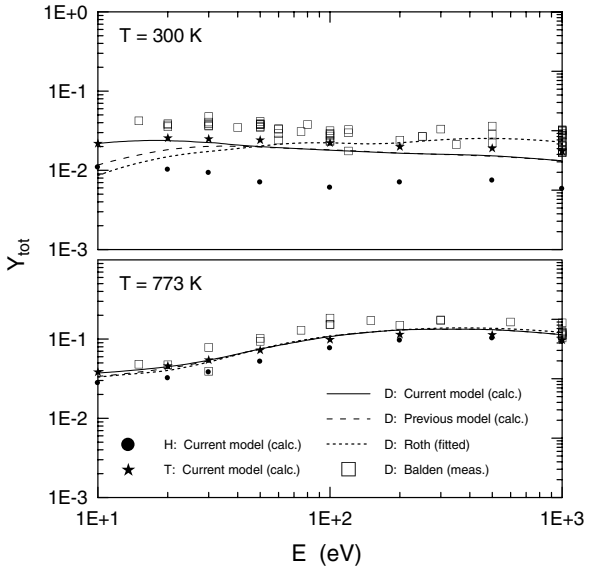

Fig. 2. Y_{tot} as a function of ion energy for graphite bombarded by hydrogen isotope ions at target temperatures of 300 and 773 K.

Another consequence of the modified surface C concentration due to hydrogen bombardment is the variation of the surface binding energy [22], which is taken into account in TRIDYN but not in TRIM.SP. Therefore, the threshold ion energy, which has to be overcome for physical sputtering (E_{thres}), is – in addition to the isotope dependence – target temperature dependent. In this study, E_{thres} is the ion energy at which Y_{phys} equals 10^{-4}. At a target temperature of 300 and 773 K, the target temperature dependent value of E^{calc}_{thres} is 43.2 and 44.1 eV for H; 28.1 and 29.2 eV for D; and 23.1 and 26.6 eV for T, respectively. The target temperature independent value of E^{Roth}_{thres} is 40.0, 32.2, and 34.2 eV for H, D, and T ion irradiations, respectively. It retains its maximum value for H ion irradiation and its minimum value for D ion irradiation.

Fig. 2 displays Y_{tot} as a function of ion energy due to D ion irradiation at target temperatures of 300 and 773 K, in which Y^{calc}_{tot}, Y^{prev}_{tot}, Y^{Roth}_{tot}, and Y^{meas}_{tot} are shown as solid lines, dashed lines, dotted lines, and open squares, respectively. The measured data Y^{meas}_{tot} are adopted from Refs. [10,14]. Basically, the results show that Y^{calc}_{tot} at both target temperatures are consistent with the corresponding Y^{Roth}_{tot} as well as Y^{meas}_{tot}. At a target temperature of 300 K and low ion energy, Y^{calc}_{tot} gets closer to Y^{meas}_{tot} than Y^{prev}_{tot} and Y^{Roth}_{tot}. This is one of the major achievements of the current simulation model by introducing the out-diffusion probability. Furthermore, the fact that when Y^{calc}_{phys} is at a high ion energy, it is smaller than that of Y^{Roth}_{phys} (as shown in Fig. 1), accounting for why Y^{calc}_{tot} is smaller than Y^{Roth}_{tot}.

Also shown in Fig. 2 are Y^{calc}_{tot} versus ion energy for H (circles) and T (stars) ion irradiation at target temperatures of 300 and 773 K for comparison to D. As can be seen, T and H ions have the largest and smallest values of Y^{calc}_{tot}, respectively. The discrepancies among Y^{calc}_{tot} for H, D, and T are significantly reduced as target temperature increases but insignificantly reduced as ion energy increases.

Fig. 3 shows Y_{chem} as a function of target temperature at 50 and 100 eV D ion irradiation, and compares Y^{calc}_{chem}, Y^{prev}_{chem}, Y^{Roth}_{chem}, and Y^{meas}_{chem}. The measured data Y^{meas}_{chem} are adopted from the weight loss

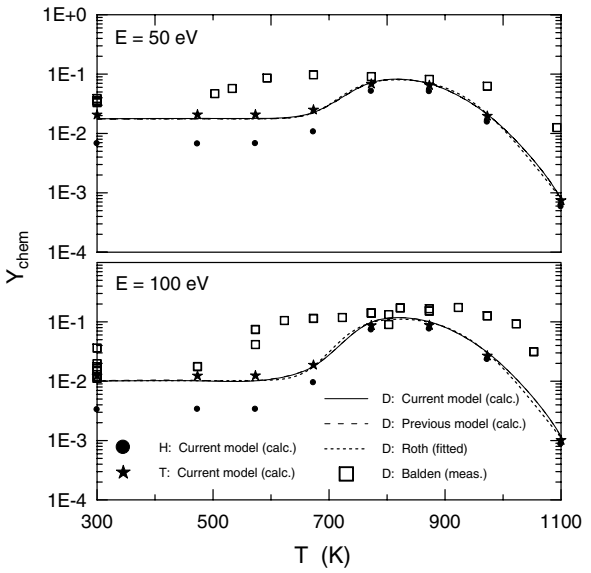

Fig. 3. Y_{chem} as a function of target temperature for graphite bombarded by hydrogen isotope ions at ion energies of 50 and 100 eV.

measurements from Refs. [10,14]. As can be seen, all of Y^{calc}_{chem}, Y^{prev}_{chem}, Y^{Roth}_{chem}, and Y^{meas}_{chem} values are close to each other. Especially, the Y^{calc}_{chem} and Y^{prev}_{chem} values are almost the same and hard to be singled out. In addition, Y_{chem} exhibits the well-known maximum at high target temperatures for ion energies of 50 and 100 eV. This is due to the thermally activated process and is described in detail in Refs. [1,3,10,26]. The peak target temperature (T^{peak}_{chem}) is the temperature at which Y_{chem} reaches its maximum. The T^{peak}_{chem} values for both ion energies of 50 and 100 eV and all three hydrogen isotopes are at approximately 800 K. Nevertheless, the measured data show a much broader peak, a shift of the maximum [10], and slightly higher values. None of the models describes this experimental observation.

Fig. 3 also compares Y^{calc}_{chem} against target temperature for H (circles), D (solid lines), and T (stars) ion irradiation at ion energies of 50 and 100 eV. As shown, T and H ions hold the largest and smallest values of Y^{calc}_{chem}, respectively. Note, the discrepancies among Y^{calc}_{chem} for H, D, and T are also significantly reduced as target temperature increases but insignificantly reduced as ion energy increases.

4. Conclusions

This study has successfully developed a comprehensive computer model to simulate chemical erosion of graphite due to hydrogen isotope ion irradiation. The calculated results correlate more closely to measured data than the fitted ones by Roth. Both, physical sputtering and chemical erosion yields, vary with ion energy, target temperature, and ion mass. However, the target temperature at which chemical erosion yield reaches its maximum is nearly independent of ion energy and ion mass. As a whole, the isotope effect has influence on: (1) the surface-related coefficient; (2) the thermally activated coefficient; (3) the threshold ion energy for physical sputtering. Among them, the surface-related coefficient shows a stronger target-temperature dependence than the thermally activated coefficient. Among all three hydrogen isotopes, deuterium and hydrogen ions have the largest surface-related and thermally activated coefficients, respectively. The threshold ion energy for physical sputtering increases with higher target temperature, but decreases with greater ion mass.

Acknowledgements

The authors would like to thank Dr W. Jacob for stimulating many valuable discussions. This study was financially supported by the Max-Planck-Institute for plasma physics (Federal Republic of Germany) and the National Science Council (Republic of China).

References

[1] J. Roth, C. García-Rosales, Nucl. Fusion 36 (1996) 1647, with corrigendum Nucl. Fusion 37 (1997) 897.
[2] R. Parker, G. Janeschitz, H.D. Pacher, D. Post, S. Chiocchio, G. Federici, P. Ladd, ITER Joint Central Team, Home Teams, J. Nucl. Mater. 241–243 (1997) 1.
[3] J. Roth, J. Nucl. Mater. 266–269 (1999) 51.
[4] E. Vietzke, K. Flaskamp, V. Philipps, G. Esser, P. Wienhold, J. Winter, J. Nucl. Mater. 145–147 (1987) 443.
[5] A.A. Haasz, J.A. Stephens, E. Vietzke, W. Eckstein, J.W. Davis, Y. Hirooka, in: Atomic and Plasma-Material Interaction Data for Fusion 7A, International Atomic Energy Agency (IAEA), Vienna, Austria, 1998.
[6] B.V. Mech, A.A. Haasz, J.W. Davis, J. Nucl. Mater. 255 (1998) 153.
[7] E. Vietzke, J. Nucl. Mater. 290–293 (2001) 158.
[8] R.G. Macaulay, A.A. Haasz, J.W. Davis, J. Nucl. Mater. 337–339 (2005) 857.
[9] M. Balden, C. Adelhelm, E. de Juan Pardo, J. Roth, J. Nucl. Mater., these Proceedings, doi:10.1016/j.jnucmat.2007.01.188.
[10] M. Balden, J. Roth, J. Nucl. Mater. 280 (2000) 39.
[11] R. Schwörer, H. Plank, J. Roth, J. Nucl. Mater. 241–243 (1997) 1156.

[12] J.H. Liang, M. Mayer, J. Roth, W. Eckstein, Nucl. Instrum. Meth. B 202 (2003) 195.
[13] C. Hopf, A. von Keudell, W. Jacob, J. Appl. Phys. 94 (2003) 2373.
[14] M. Balden, J. Roth, unpublished data.
[15] D.K. Brice, B.L. Doyle, W.R. Wampler, J. Nucl. Mater. 111 & 112 (1982) 598.
[16] W. Möller, B.M.U. Scherzer, J. Appl. Phys. 64 (1988) 4860.
[17] W. Möller, J. Nucl. Mater. 162–164 (1989) 138.
[18] W. Möller, B.M.U. Scherzer, Appl. Phys. Lett. 50 (1987) 1870.
[19] J. Roth, J. Bohdansky, N. Poschenrieder, M.K. Sinha, J. Nucl. Mater. 63 (1976) 222.
[20] C. García-Rosales, J. Roth, J. Nucl. Mater. 196–198 (1992) 573.
[21] M. Balooch, D.R. Olander, J. Chem. Phys. 63 (1975) 4772.
[22] W. Möller, W. Eckstein, J.P. Biersack, Comput. Phys. Commun. 51 (1988) 355.
[23] C. Hopf, W. Jacob, J. Nucl. Mater. 342 (2005) 141.
[24] J.P. Biersack, W. Eckstein, Appl. Phys. A 34 (1984) 73.
[25] P.W. Atkins, Physical Chemistry, 5th Ed., Oxford University, Oxford, United Kingdom, 1994.
[26] J. Biener, U.A. Schubert, A. Schenk, B. Winter, G. Lutterloh, J. Kűppers, J. Chem. Phys. 99 (1993) 3125.